

Novel Hybrid Materials Of Cellulose Fibres And Nanoparticles

A. C. Small*, J. H. Johnston*

*Victoria University of Wellington and The MacDiarmid Institute for Advanced Materials and Nanotechnology, Wellington, New Zealand, jim.johnston@vuw.ac.nz

ABSTRACT

Hybrid materials are of interest due to the potential synergistic properties that may arise from the combination of two or more precursors. Such precursors are paper fibres (cellulose) and magnetic or photoluminescent nanoparticles. These materials exhibit the inherent properties of the substrate, in particular flexibility and strength, and also the properties of the surface bonded nanoparticles.

Keywords: cellulose, nanoparticles, magnetic, photoluminescent.

1 INTRODUCTION

Cellulose, $(C_6H_{10}O_5)_n$, is a long-chain polymeric carbohydrate of β -glucose. It is the fundamental structural component of green plants, in which the primary cell wall of the plant is predominantly cellulose, and the secondary wall contains cellulose with variable amounts of lignin. Lignin and cellulose, considered together, are termed lignocellulose, which (as wood) is the most common biopolymer on earth. Cellulose monomers (β -glucose) are linked together through 1,4 glycosidic bonds by condensation. Each monomer is oriented 180° to the next, as seen in figure 1 below, and the chain is built up two units at a time.

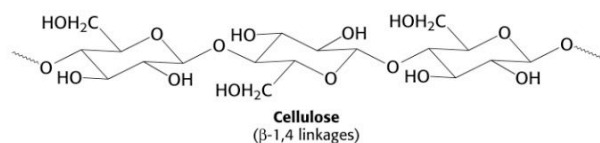


Figure 1: Structure of cellulose $(C_6H_{10}O_5)_n$.

The cellulose chains are formed into micro fibrils that constitute the basic framework of the plants cell. In micro fibrils, the multiple hydroxyl groups on the glucose units hydrogen bond with each other, holding the chains firmly together and contributing to their high tensile strength [1]. Cellulose and its derivatives (paper, nitrocellulose, cellulose acetate, etc.) are principal materials generated by industry and see a considerable economic investment. Magnetically responsive cellulose fibres allow the investigation of new concepts in papermaking and packaging, security paper, and information storage. Potential applications are in electromagnetic shielding,

magneto-graphic printing and magnetic filtering. Doped ZnS nanoparticles have attracted large amounts of interest since 1994 when Bhargava et al [2]. reported for the first time that Mn^{2+} doped ZnS could yield high quantum luminescence efficiency. As well as ZnS:Mn nanoparticles, a large amount of work has been dedicated to investigating the synthesis and properties of copper doped ZnS nanoparticles. The combination of doped ZnS nanoparticles and cellulose fibres could lead to the development of new security papers and cost effective display technology.

2 EXPERIMENTAL

Magnetite (Fe_3O_4) nanoparticles were synthesized by adding aqueous ammonia drop wise from a burette to solutions containing dissolved $FeCl_2 \cdot 4H_2O$. Black precipitates were formed immediately [3]. As particle size is dependant on both the concentration of the precursor solution and the rate precipitation, various concentrations of precursor solution were used and the precipitation rate was kept constant. These are summarized in table 1.

In a typical synthesis of Mn^{2+} or Cu^{2+} doped ZnS particles, $ZnCl_2$, $MnCl_2$ or $CuCl_2$ and sodium citrate solution were mixed and stirred at constant speed for 10 minutes. From a burette, Na_2S was added drop wise. A white precipitate was formed immediately. The resulting suspension was centrifuged and then washed with distilled water.

A colloidal suspension of these nanoparticles was then added to an approx. 2 wt. % suspension of bleached *pinus radiata* Kraft paper fibres and stirred vigorously for approximately 2 hours, after which they were filtered and washed with H_2O . The resultant coated fibres were then sonicated for 20 minutes in order to remove any loosely bound nanoparticles.

3 RESULTS AND DISCUSSION

3.1 Magnetic Nanoparticles

Pinus radiata Kraft fibres coated with Fe_3O_4 nanoparticles retain the inherent properties of the fibre; tensile strength, flexibility, and the ability to be made into a sheet. The fibres also gain the magnetic properties of the surface bound nanoparticles. Consistent with the literature [8], particle size decreases as the concentration of $FeCl_2 \cdot 4H_2O$ decreases. X-ray line broadening indicates that samples have an average particle size of between 12 and 26

nm, depending on solution concentration. By varying the concentration of Fe^{2+} in the precursor solution, different particle sizes were obtained (table 1).

Solution conc. (%)	Average particle size (nm)	Saturation magnetisation (emu g^{-1})	Coercive field (Oe)
3.00	26	62	112
0.60	24	62	122
0.05	15	70	42
0.025	12	63	19

Table 1: Effect of precursor solution concentration on particle size, saturation magnetisation and coercive field of Fe_3O_4 nanoparticles.

Magnetisation versus applied field curves are presented in figures 2 and 3.

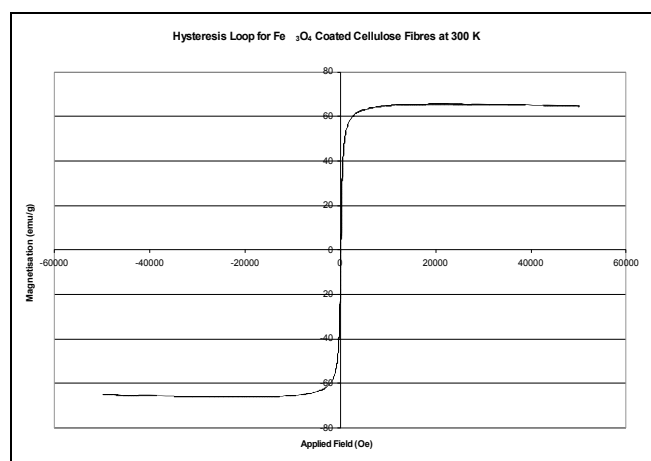


Figure 2: Magnetic hysteresis loop for Fe_3O_4 -coated cellulose fibres at 300 K. Sample has an Fe loading of 2.88 %.

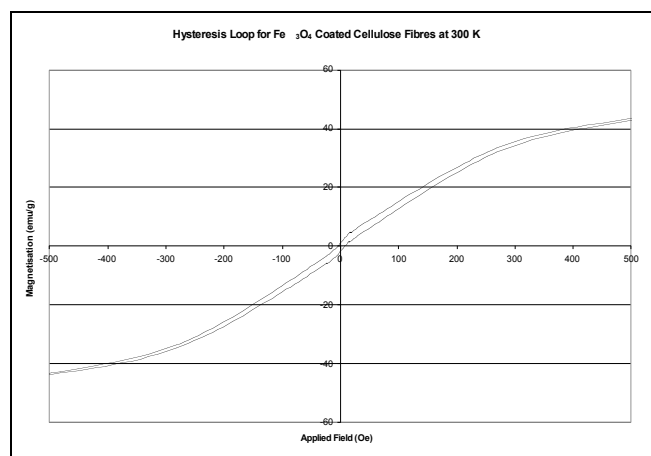


Figure 3: Magnified view of Fe_3O_4 hysteresis loop at 300 K. A small remnant magnetization is visible.

Saturation magnetisation is independent of particle size but dependent on temperature. Fe_3O_4 -coated cellulose fibre samples show a saturation magnetisation of $\sim 65 \text{ emu g}^{-1}$. This value is comparable to the values of saturation magnetisation of bulk Fe_3O_4 , indicating that the combination of cellulose fibres and magnetic nanoparticles does not alter the magnetic properties of the nanoparticles. The magnetic moment is also comparable to materials with similar Fe_3O_4 loadings [4]. Lowering the concentration of Fe^{2+} in the precursor solution results in the formation of smaller particles, and changes the coercive field accordingly. Particle sizes calculated using the Debye-Scherrer approximation for XRD are only average particle sizes, hence a smaller average particle size means a larger number of particles will be in the superparamagnetic range, and as a consequence, the coercive field is lowered. Coercive fields at 300 K for these materials are very low; $H_c = \sim 20\text{-}120 \text{ Oe}$. A coercive field as low as this is ideal for application in electromagnetic shielding. The materials also possess small remnant fields of $\sim 3\text{-}11 \text{ emu g}^{-1}$ at 300 K, as shown in the magnetic hysteresis loops in figures 2 and 3 above. Optical microscope images show that the coated fibres retain the same morphology as the precursor Kraft fibres. The brown colour of the fibres (a change from the original white) indicates they are coated with the Fe_3O_4 nanoparticles. From the SEM image shown in figure 4, the completeness of the coating can be seen. The Fe_3O_4 nanoparticles completely encapsulate the fibre and follow its morphology, similar to previous research involving cellulose fibres coated with conducting polymers [5].

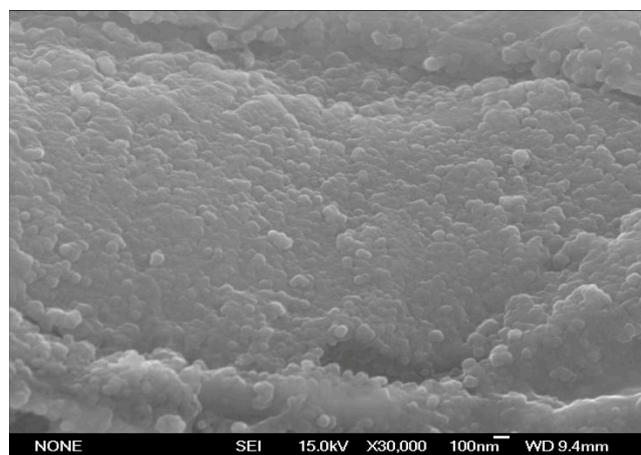


Figure 4: SEM images of Fe_3O_4 cellulose fibres.

This is also confirmed by examining the EDS map for Fe (figure 5), which shows full coverage of the fibre surface. Nanoparticles are present on the surface of the cellulose fibres in agglomerations of $\sim 100 \text{ nm}$, as no surfactant was used in the synthesis procedure. This differs from the particle size calculated using the Debye-Scherrer approximation, where the individual crystallite size was calculated as being between 12-26 nm. XRF analysis shows the samples to be 0.5-2.8 % Fe. The $\text{Fe } 2p$ XPS spectrum of

the Fe_3O_4 nanoparticles (Figure 6) shows the Fe_3O_4 and $\alpha\text{-FeOOH}$ phases to be present [6], consistent with XRD results. A comparison between the Fe 2*p* XPS spectrum of Fe_3O_4 coated cellulose fibres and Fe_3O_4 nanoparticles (figure 7) shows a considerable shift to lower binding energy of up to 1.5 eV for both the 1/2 and 3/2 spin multiplicities of the coated samples. This shift confirms that there is chemical bonding between the Fe_3O_4 nanoparticles and the cellulose fibre surface, presumably through hydrogen bonding between the O in the Fe_3O_4 and $\alpha\text{-FeOOH}$ nanoparticles and the H of the OH groups present in cellulose. The shape of the Fe 2*p* XPS spectrum of Fe_3O_4 -coated cellulose fibres does not change compared to that of the Fe_3O_4 nanoparticles by themselves. This indicates that the chemical bonding between the Fe_3O_4 nanoparticles and the cellulose fibre does not alter the chemistry of the nanoparticles. Even after repeated washing and sonication steps, the particles remain bound to the surface. This is contrary to other reports in the literature which state that particles on the fibre surface are removed in the washing step

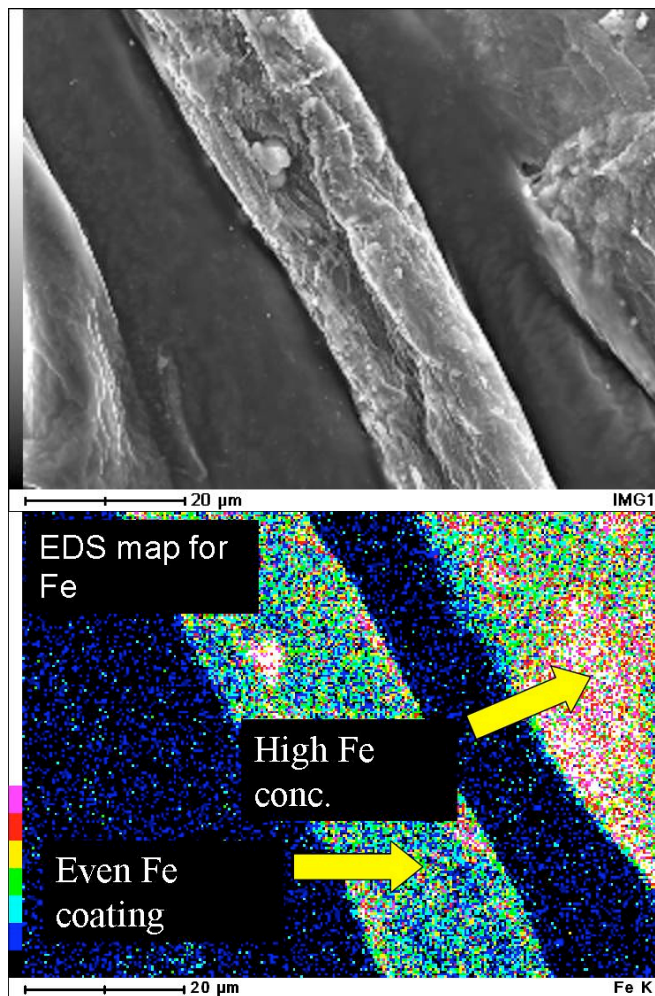


Figure 5: EDS images of Fe_3O_4 coated cellulose fibres, SEI image (above) and elemental Fe map (below).

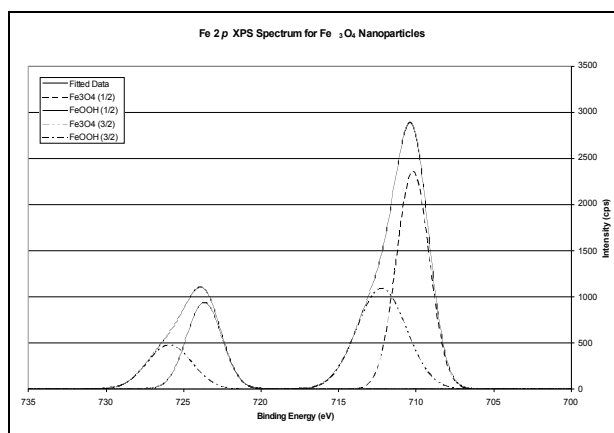


Figure 6: XPS spectrum of Fe_3O_4 nanoparticles.

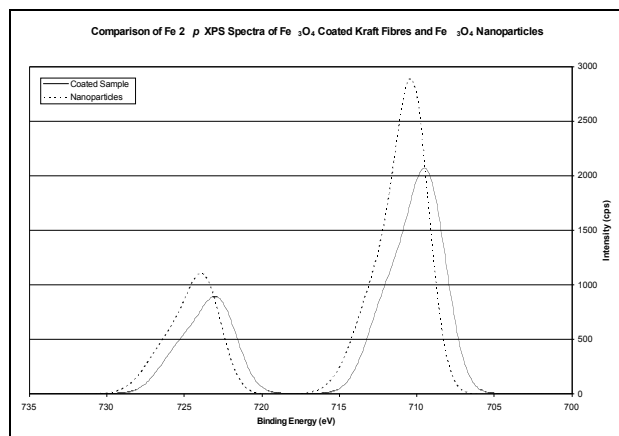


Figure 7: Comparison between Fe 2*p* XPS spectra of Fe_3O_4 -coated Kraft fibres and Fe_3O_4

3.2 Photoluminescent Nanoparticles

Figure 8 shows the photoluminescence emission spectrum of ZnS:Mn powders synthesized by the aforementioned methods.

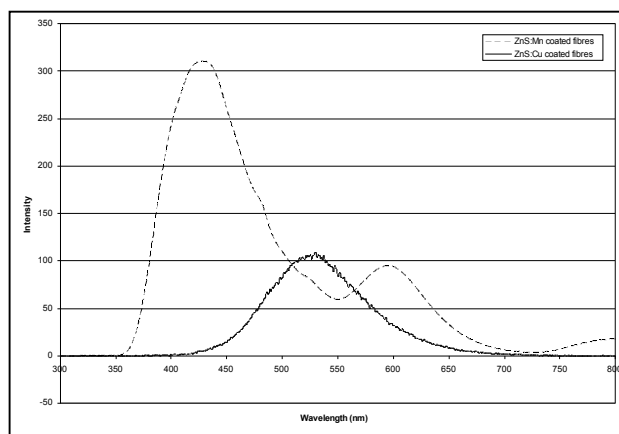


Figure 8: Photoluminescence emission spectra of doped ZnS nanoparticles.

An emission peak can be seen at approximately 590 nm, which can be attributed to the ${}^1A_g \rightarrow {}^2T_g$ transition in Mn^{2+} . The larger peak at 480 nm can be attributed to an emission due to S^{2-} vacancies in the ZnS lattice [7]. In the case of ZnS:Cu, a broad blue-green emission can be seen at approximately 520 nm. The source of this emission has been fiercely debated. A recent theory suggests the emission arises from the transition of an excited electron from an S^{2-} vacancy in the ZnS lattice to the t_{2g} excited state of the Cu^{2+} [8]. Again, on bonding to cellulose fibres, the emissions are unaffected. X-ray photoelectron spectroscopy (XPS) shows that bonding is occurring between the doped ZnS nanoparticles and the cellulose surface, due to shifts in the 3/2 and 1/2 spin multiplicities of the 2p electrons of both Zn and S. In some cases the shift is large up to 1.4 eV (figure 10).

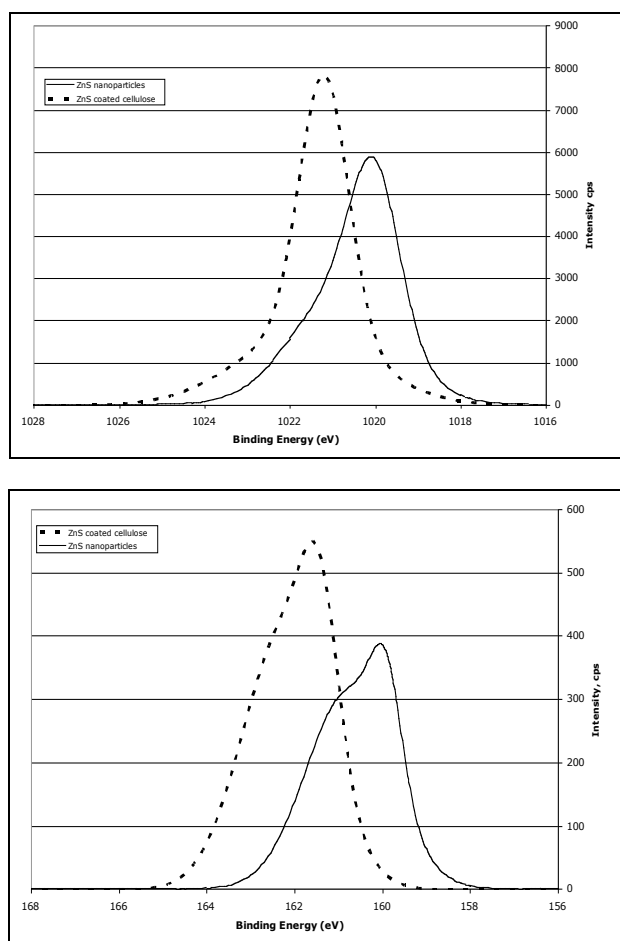


Figure 10: XPS spectra for 2p electrons in ZnS:Mn nanoparticles and ZnS:Mn coated cellulose fibres. Zn 2p above, and S 2p below.

On examining electron microscope images (figure 11), it can be seen that spherical nanoparticles of doped ZnS have been formed. It is difficult to deduce particle size from these images as the particles have agglomerated due to the

absence of a surfactant during the synthesis procedure. From x-ray line broadening analysis, the average particle size is ~ 15 nm for both ZnS:Mn and ZnS:Cu nanoparticles. Electron dispersive spectroscopy (EDS) indicates that the particles are indeed ZnS, and in both cases, the dopant can be mapped as well.

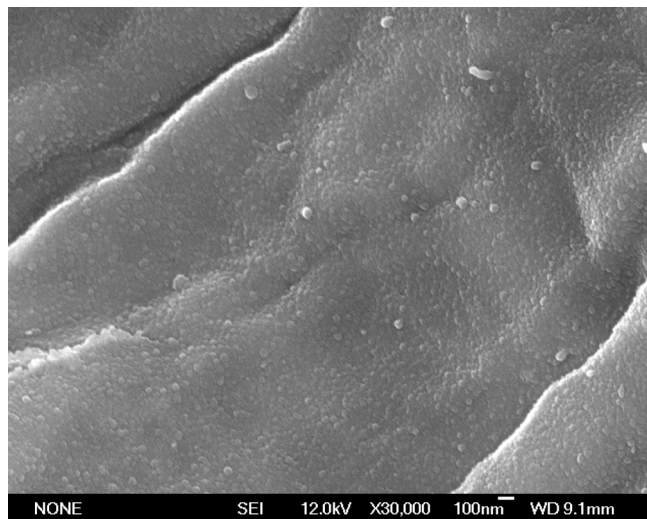


Figure 11: SEM micrograph showing the surface of the cellulose fibre coated with ZnS:Mn nanoparticles

4 CONCLUSIONS

Fe_3O_4 and Cu^{2+} and Mn^{2+} doped ZnS nanoparticles were synthesized and hybrid materials of these and cellulose fibres were prepared and characterized using a number of techniques. It has been shown that the nanoparticles coat the surface evenly and retain the magnetic and photoluminescent properties of their standalone powders.

REFERENCES

- [1] Wallenberrger and Weston, "Natural fibers, polymers and composites.", Kluwer Academic Publishers, 2004.
- [2] R. N. Bhargava, D. Gallagher, X. Hong, A. Nurmikko, *Phys. Rev. Lett.*, 72, 416, 1994.
- [3] P. Berger, N. B. Adelman, K. J. Beckman, D. J. Campbell, A. B. Ellis, G. C. Lisensky, *J. Chem. Ed.*, 76, 943, 1999.
- [4] R. H. Marchessault, P. Rioux, L. Raymond, *Polymer*, 33, 4024, 1992.
- [5] M. J. Richardson, J. H. Johnston, T. Borrmann, *Curr. Appl. Phys.* 6, 462, 2006.
- [6] J. F. Anderson, M. Kuhn, U. Diebold, *Surf. Sci. Spectra*, 4, 266, 1998.
- [7] L. Sun, C. Liu, C. Liao, C. Yan, *J. Mater. Chem.* 9, 1655, 1999.
- [8] P. Yang, M. Lu, D. Xu, G. Zhou, *Appl. Phys. A*, 73, 455, 2001.